npj | flexible electronics

Published in partnership with Nanjing Tech University

Article

https://doi.org/10.1038/s41528-025-00449-w

A universal method for constructing stretchable and conductive connections in flexible electronics

Yahui Zhao, Qiyang Ruan, Tongtong Li, Hongyun Qiu, Ruipeng Zhang, Shuai Wen, Lifeng Chi ✉ & Shaobo Ji ✉

Integrating stretchable and rigid electric units presents a significant challenge in manufacturing stretchable electronics. Their surface property differences prevented reliable stretching-tolerant connections. Here, we report a universal method to construct stretchable connections based on interfacial covalent reactions. It enables robust and conductive bonding among various soft/rigid electronics through simple surface modification and interfacial reaction. The bonding between SEBS rubber and metals reached stretchability over 250% with interfacial toughness over 200 N/m. The ultrathin connection layer provided conductive pathways, achieving an electrical stretchability of 60% between Au-deposited SEBS and Cu sheets. Connections between liquid metal-based stretchable conductors could withstand more than 10,000 stretching cycles to 60% strain while maintaining their high conductivity. The versatility and stability of this method were further proved by fabricating electronic devices that integrated soft and rigid units, including circuits on papers and a gesture-visualizing glove with LEDs, highlighting the robustness of the stretchable connections.

Flexible electronic devices have emerged in recent years, offering higher design flexibility, better adaptability[1–5], and a broader range of machinery applications[6–10]. Unlike traditional rigid electronics, flexible devices can withstand certain deformation without compromising their performance[11–13]. Among them, fully stretchable electronics are of particular interest for wearable sensors in healthcare management[14–17], as they can conformally adhere to irregular surfaces, especially the human body[18–21]. Yet, to achieve comprehensive functions, conventional silicon-based rigid chips and printed circuit boards (PCBs) remain irreplaceable due to their performance and mature manufacturing[22,23]. Currently, commercial PCBs are produced on flexible plastics[24,25], but not on stretchable materials. Consequently, flexible hybrid electronic devices that combine soft stretchable units and rigid electronic units become unavoidable in the development and application of flexible electronics. However, the connections between stretchable units and flexible/rigid electronics are crucial weaknesses in integrated flexible hybrid devices due to their poor interfacial bonding[26–29], which would easily fracture when stretched. The mechanical property differences would induce strain/stress concentration at the soft-rigid interfaces, leading to early failure during deformation, and the chemical property differences would result in low binding strength at the interfaces, causing easy detachment. The former issue could be solved by introducing mechanical gradients or rigid islands[30–32], while there were only limited solutions for the latter issue with certain shortcomings.

The connections between soft and rigid units are desired to be like the welding (irreversible) or soldering (reversible) of metals, which achieve both robust mechanical strength and stable electrical pathways. Existing connections typically use rigid or thick adhesive layers, such as conductive pastes that[33] lack stretchability after curing, induce additional mechanical differences, and apply to limited materials. Liquid metals[34,35], with outstanding mechanoelectrical properties, are also used for flexible connections. However, their high surface tension and low mechanical adhesion result in indiscriminate sticking to target materials and surrounding objects[36]. Anisotropic conductive films[37,38] are another choice, but their additional thickness makes them unsuitable for ultra-thin electronics[39], their construction is also complicated with high cost. Moreover, the applicable materials are still limited[40,41].

Therefore, developing a connection method that ensures high mechanical strength and electrical conductivity, which is also convenient and universal to the materials used in flexible electronics, is still a significant challenge. Here, we report a universal and straightforward method for achieving “stretchable welding” between various soft and rigid units (Fig. 1a). By using thiol click interfacial connection (TCIC) to covalently bond the surfaces of various materials (including rubbers, plastics, metals, etc.), their chemical differences were overcome, and rapid connections could be established. The “welded” SEBS rubber and metals reached stretchability

State Key Laboratory of Bioinspired Interfacial Materials Science, Institute of Functional Nano & Soft Materials (FUNSOM), Soochow University, Suzhou, China.
✉e-mail: chilf@suda.edu.cn; sbji@suda.edu.cn

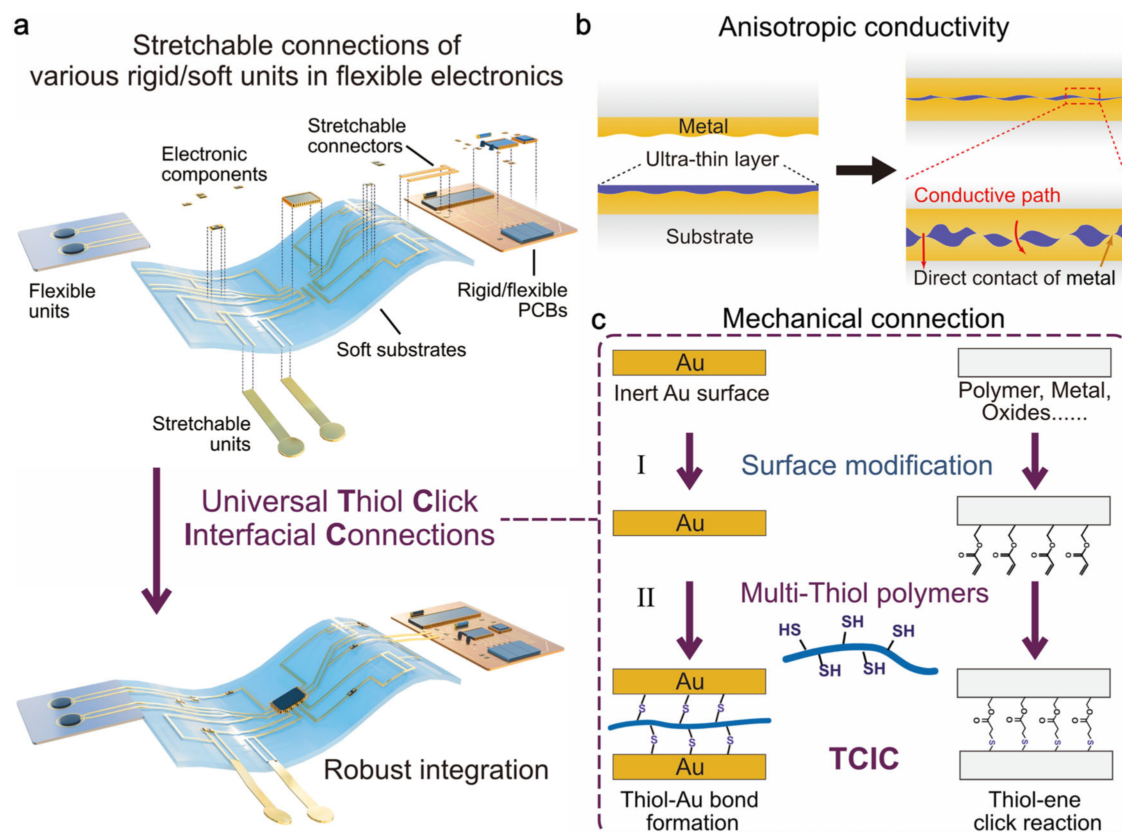

Fig. 1 | Stretchable thiol click interfacial connection (TCIC). **a** Stretchable connections of various materials and units for the integration of flexible hybrid electronics. **b** Anisotropic conductivity of the stretchable connection. **c** Schematic illustration of surface modifications and interfacial reactions during TCIC.

over 250% with interfacial toughness over 200 N/m. The nanometer-thick connection layer would not only keep the original mechanical properties of the connected materials but also provide anisotropic conductivity without conductive fillers (Fig. 1b). Electrical stretchability over 50% between Au-deposited SEBS and metals in electronics was realized, and the electrical connections stayed stable for more than 3000 stretching cycles. When liquid metal-coated PDMS was used as stretchable conductors, the stretchable connection kept stable and high conductivity during and after 10,000 stretching cycles at 60% strain. These characteristics of TCIC open new pathways for the integration of multi-material devices.

Results

Design of the universal interfacial connections

For reactions on surfaces or at interfaces, salinization after plasma treatment is one of the most convenient methods. However, plasma treatment is not suitable for Au, a frequently used material in flexible electronics. Nevertheless, Au is well known to react with thiols or disulfides to form Au-S bonds, which provide covalent connections with Au surfaces. Based on this idea, the universal interfacial connection strategy was proposed and optimized (Fig. 1c). The units/components for flexible hybrid electronics first underwent a two-step surface modification: plasma treatment and salinization. After the modification, the inert Au surface remained unaffected, while other surfaces were covalently grafted with acrylate groups. Then, multi-thiol polymers (MTPs, Fig. S1a) were used as interfacial connectors, which could form thiol-Au bonds and undergo thiol-ene click reactions, thus realizing the covalent interfacial connections that were named “thiol click interfacial connection”. TCIC was applicable to most materials used in flexible and conventional electronics, including rubbers, plastics, metals, oxides, and even papers.

The conditions for TCIC were quite mild and simple; the first surface modification was realized by air plasma treatment for 30 s, followed by vapor-phase modification with 3-(trimethoxysilyl)propyl acrylate at rt for 24 h (Fig. S2a). Then the interfacial connection was achieved by applying MTP solution with sodium ethoxide as the catalyst, contacting the surfaces, and reacting at mild temperatures (rt to 60 °C). As the amount of interfacial MTPs was low, it would not fully block the metal surfaces, thus keeping the electrical conductivity between the conductor surfaces.

Interfacial bond formation

To validate the formation of covalent bonds between surfaces during TCIC, MTP was used to connect various materials used in flexible electronics. First, PDMS was selected to confirm the surface modification and interfacial thiol-ene click reactions. The modification of acrylate groups was evidenced by contact angle measurements (Fig. S2b). Further experiments confirmed that this step would not affect the electrical and mechanical properties of the treated materials (Fig. S3). When MTP was applied, only surface-modified PDMS films were connected (Fig. 2a), which confirmed that the thiol-ene click reaction occurred and the MTP itself did not function as an adhesive. The conditions of TCIC were unified as 100 mg/ml MTP solution in acetone, 1.5 h placement at 60 °C with 0.5 kPa pressure, for reliable comparison among different material combinations (Fig. S4). Under the same condition, commercial anisotropic conductive film adhesive (3 M ACF 7303) provided interfacial toughness of ~3 N/m for PDMS, much lower than the TCIC (over 20 N/m). Besides, after 24 h placement at rt without heating, the interfacial toughness could reach similar values as 1.5 h placement at 60 °C (Fig. S4b), indicating that in practical applications, TCIC could be very mild and convenient.

Cu sheets were further used to confirm TCIC on Au surfaces. Cu and Au-coated Cu (Au@Cu) were surface-treated as in the TCIC process; bare Cu sheets that were only plasma-treated were also tested. As shown in Fig. 2b, the Au-coated Cu sheets had increased connection strength than acrylate-modified Cu. The characteristic peaks at the 240–270 cm^{-1} band in

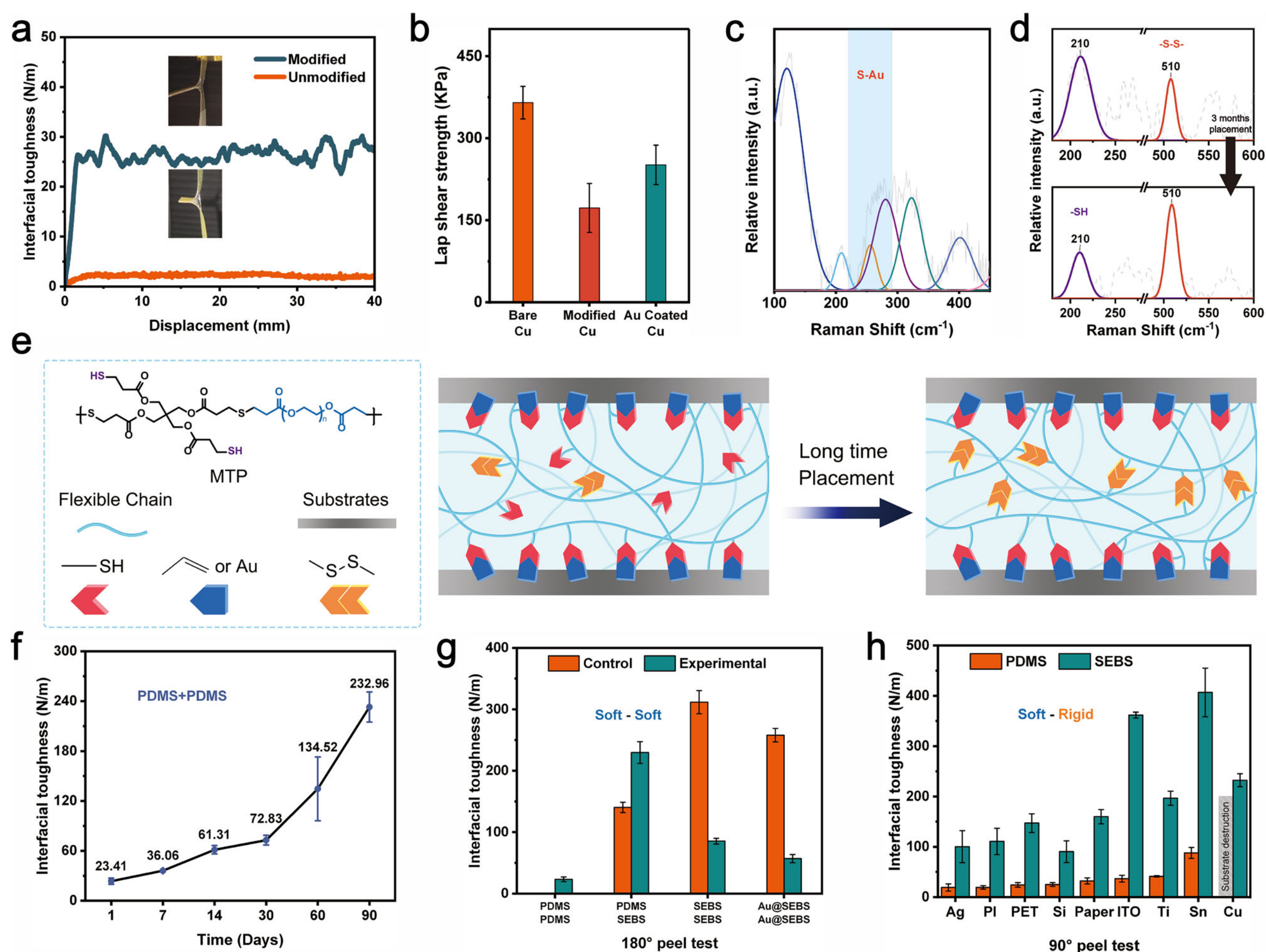

Fig. 2 | Covalent bond formation at the interfaces during TCIC. a Interfacial toughness of surface-modified and unmodified PDMS films connected by MTP after 1.5 h reaction at 60 °C. **b** Lap shear tests of Cu sheets with different surfaces. **c**, Raman spectrum of MTP-coated Au@SEBS surface, confirming the formation of thiol-Au bonds. **d** Changes in the Raman spectra of MTP before and after 3 months of storage at 4 °C. 210 cm^{-1} stood for the thiol group, and 510 cm^{-1} stood for disulfide bonds. **e** Illustration of the covalent bonds formed at interfaces connected by TCIC. The conversion from thiols to disulfides at rt could continuously strengthen the interfaces. **f** The interfacial toughness of TCIC-connected PDMS films gradually enhanced with prolonged rt placement. **g** 180° peel tests of soft-soft combinations. The PDMS + PDMS combination had almost 0 interfacial toughness. Au@PDMS was not shown as the Au layer would easily detach from PDMS and result in almost 0 interfacial toughness. **h** 90° peel tests of soft-flexible/rigid combinations with PDMS or SEBS as the soft stretchable materials. The PDMS + Cu combination had high interfacial toughness, and the PDMS film fractured early during the peeling tests; thus, their toughness values were not obtained.

the Raman spectrum confirmed the existence of thiol-Au bonds (Fig. 2c). The surface of bare Cu was oxidized during plasma treatment and could better react with thiol groups to form thiol-Cu bonds (bond energy of Cu-S is 274.5 ± 14.6 kJ/mol, Au-S is 253.6 ± 14.6 kJ/mol)[42], leading to the highest connection strength. The acrylate-modified Cu had a lower reaction site density than bare metals and thus had the lowest strength. Nevertheless, all three groups were well connected by TCIC.

The surface acrylate groups were a monolayer, so the thiol-ene reaction would quickly be "saturated". The excess thiol groups in the MTP would then be slowly oxidized into disulfide bonds. The Raman spectra of MTP samples confirmed the oxidation (Fig. 2d). The characteristic peak of thiol groups appeared at 210 cm^{-1}, and the disulfide bond peak appeared at 510 cm^{-1}. After storing it for 3 months, the ratio of disulfides to thiols significantly increased, indicating continuous interfacial bond formation after the initial connection by TCIC (Fig. 2e). It was also validated by the self-strengthening interfaces in TCIC-connected PDMS. With longer placement times, the interfacial toughness continuously increased and reached about 233 N/m after 3 months (Fig. 2f). Moreover, even after self-strengthening, the physical properties of the connected materials would not be affected (Fig. S5), which was beneficial for applications in flexible electronics.

Mechanical strength and stretchability

The interfacial toughness of different material combinations was measured to validate the universality of TCIC. PDMS and SEBS were selected as typical materials for soft-soft connections (Fig. 2g). For combinations with PDMS, the interfacial toughness was significantly improved compared to almost 0 without TCIC. Due to the excellent self-adhesion of SEBS, when SEBS or Au-coated SEBS (Au@SEBS) was connected to itself, TCIC exhibited lower interfacial toughness. However, after rt placement, their interfacial toughness increased rapidly and reached a comparable value to the SEBS control group (Fig. S6) and neutralized this issue. When SEBS was connected to other materials, TCIC still greatly enhanced the connection strength (Fig. S7a). For soft-rigid connections, PDMS and SEBS, as stretchable soft parts, were successfully connected with various rigid parts, including flexible materials PI, PET, and paper; electronic materials Cu, Ag, Ti, Sn, Si, and ITO (Fig. 2h and Fig. S7a). Contact angle tests confirmed the modification of acrylate groups on the material surfaces, suggesting that the interfacial thiol-ene reactions promoted the connections (Fig. S7b). The tough bonding of PDMS and SEBS with other materials proved that TCIC was a universal method for various materials.

The improved interfacial strength provided the possibility for robust connections between stretchable and flexible/rigid units. The connected

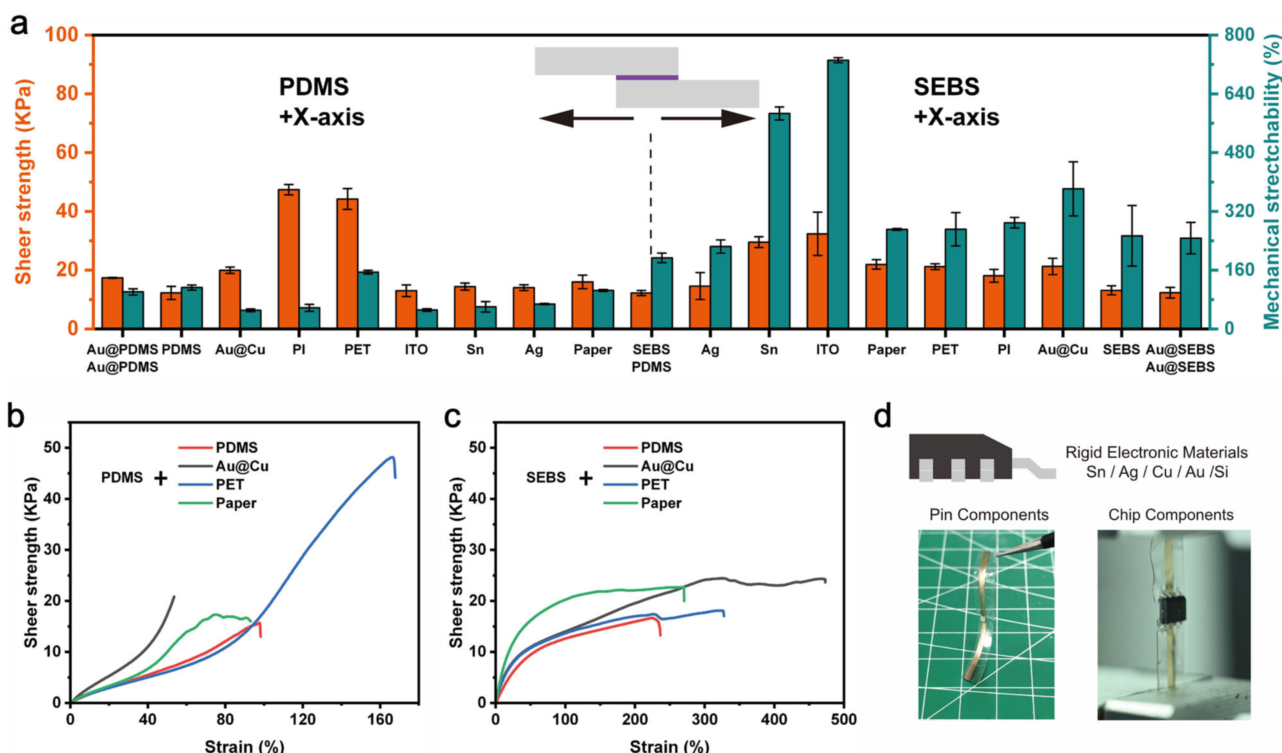

Fig. 3 | The mechanical stretchability of TCIC. a Summary of mechanical stretchability (strain at break) of TCIC-connected soft-flexible/rigid combinations. Typical tensile curves of TCIC connected. **b** PDMS, and **c**, SEBS with other materials. **d** The common materials used in electronic components, and TCIC connected electronics components with Au@SEBS stretchable conductors. Left: an LED unit bridging two Au@SEBS films. Right: a chip with 8 pins bridging two Au@SEBS films.

hybrid units kept the stretchability of the soft parts; their lap shear strength and mechanical stretchability (maximum strain) were summarized in Fig. 3a. All the combinations exhibited decent strength and acceptable stretchability, especially the SEBS combinations due to the excellent stretchability of SEBS. Typical tensile curves for the shear stretching tests were selected (Fig. 3b, c), representing the connection of PDMS or SEBS with rubbers, plastics, metals, and papers. The curves for all material combinations are in Fig. S8.

The connections of stretchable materials with materials for manufacturing conventional electronic components (metals, silica, and oxides) have already been realized by TCIC. To further confirm that TCIC could construct stable connections between stretchable circuits and electronic components, rigid LEDs and chips were connected to stretchable materials (Fig. 3d). They could be well connected and achieve high stretchability (Fig. S9). The stretchability between PDMS/SEBS and various flexible/rigid materials validated that TCIC was a universal method for constructing reliable mechanical connections.

Electrical conductivity and stretchability

Unanticipated, the added MTP layer did not block the electron pathway between the surfaces, and TCIC-connected Au@Cu kept their high conductivity (Fig. S10). More accurate measurements confirmed the low contact resistance of TCIC which was only ~1.5 mΩ with 50 mg/mL MTP and ~3.5 mΩ with 50 mg/mL MTP for 1 cm^2 contact area between Cu@PI (Fig. S11a). And the oxidation of MTP layer would not result in increased contact resistance (Fig. S11b). To understand the mechanism, the MTP interlayer was exposed by a sacrificial layer method (Fig. S12a), followed by characterization by a conductive atomic force microscope (C-AFM). As the amount of MTP was quite small (the solution applied was 0.7-0.8 μL/cm^2), the MTP interlayer was thinner than 10 nm with imperfections (Fig. 4a), leaving exposed metal surfaces. When connected, these exposed points from two surfaces contact each other and build conductive pathways (Fig. 4b), especially when one of them is a deformable soft unit. The conductivity mapping by C-AFM confirmed the leaky conductive sites in the MTP interlayer (Fig. 4c), and with less MTP the exposed conductive sites could be increased (Fig. S12b). The absence of conductive fillers guaranteed an anisotropic conductivity of TCIC, making its applications more convenient.

The electrical stretchability of TCIC was measured with Au@SEBS and liquid metal-coated PDMS (EGaIn@PDMS) (Fig. S13a). Au@PDMS is also popular, but the poor Au-PDMS interface limited their stretchability after connection (Fig. S13b). The electrical stretchability was first confirmed by connecting two Au@SEBS films (Fig. 4d). As Au@SEBS could be refined to an excellent self-connective stretchable conductor[41], the control group exhibited higher electrical stretchability. The reason was the stronger MTP-Au interface than the Au-SEBS interface. Although the Au was more tightly bonded to SEBS than to PDMS, the Au would still be peeled off from SEBS by TCIC during stretching before mechanical failure (Fig. S14a). Nevertheless, TCIC-connected Au@SEBS films showed good stability and could be further improved by using striped Au@SEBS films (Fig. S14b). Moreover, the TCIC-connected Au@SEBS exhibited better electrical stretchability in the strain range of 0-40%. As shown in Fig. S14c, even though strain/stress concentration appeared at the edges of the connection, the MTP layer also dissipated the stress of the covered Au, leading to slower and less crack formation during stretching. Further, Au@SEBS films were connected to patterned commercial Cu@PI films, which simulated the connections of stretchable units with flexible PCBs. After 3,000 stretching cycles at 40% strain, the resistance increased by only 17% at 40% strain (Fig. 4e), indicating the good stability of TCIC-connected electronics.

EGaIn@PDMS, benefiting from liquid metal, had excellent mechanoelectrical performance, but the poor adhesion of PDMS and liquid metal hindered their connection. TCIC could overcome this problem and realized robust connections for EGaIn@PDMS (Fig. 4f). The EGaIn@PDMS had to be stripped as liquid metal would easily peel off from PDMS, and bare PDMS surfaces were required to provide mechanical connections. TCIC-connected EGaIn@PDMS also exhibited excellent stability; it remained highly conductive during and after 10,000 stretching cycles at 60% strain,

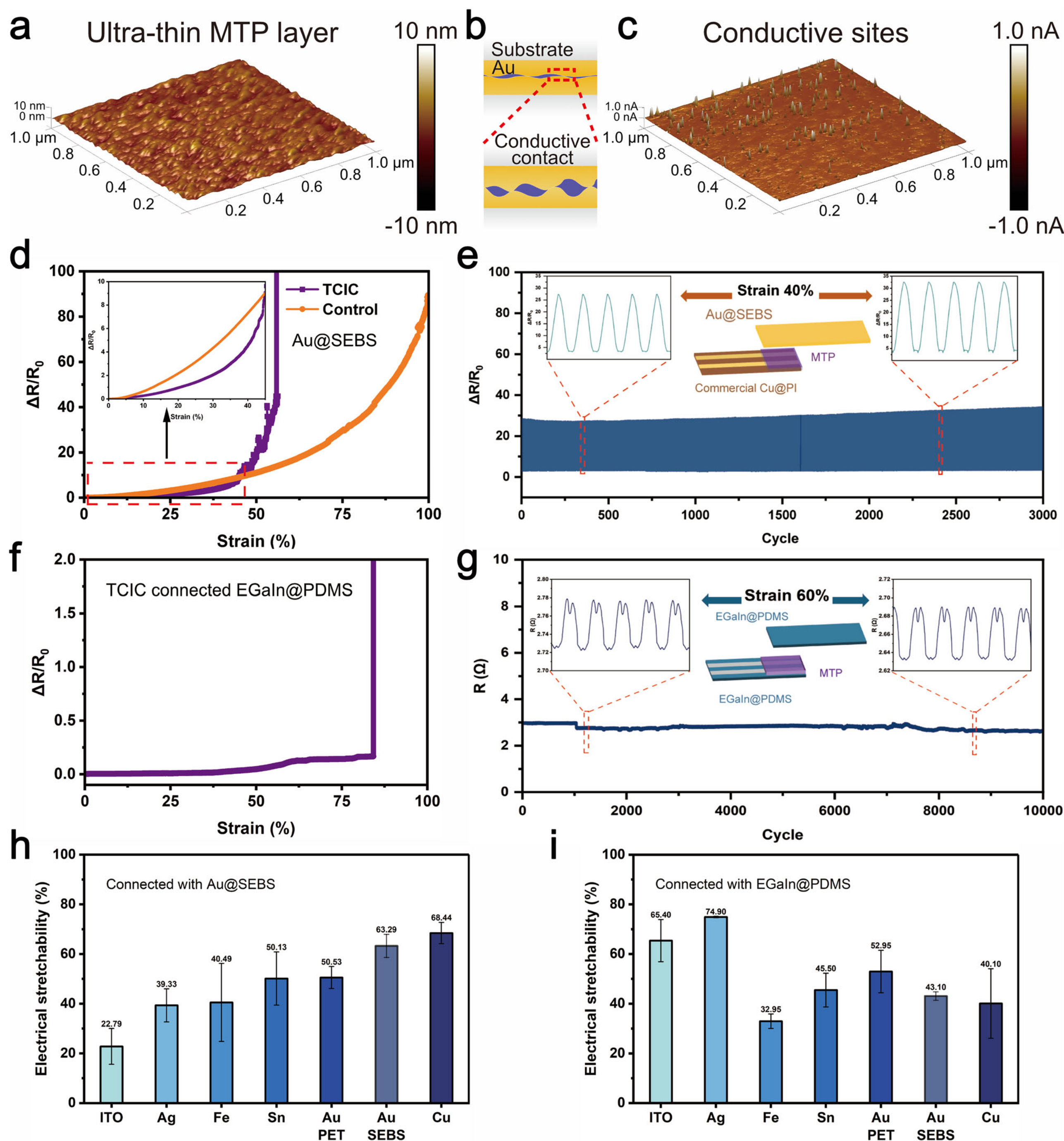

Fig. 4 | The electrical connectivity and stretchability of TCIC. **a** 3D AFM height map of exposed Au surface after TCIC treatment with 100 mg/mL MTP. **b** The mechanism for the electron pathways at the MTP interlayer after TCIC. **c** Exposed conductive sites revealed by conductive AFM. **d** Comparison of electrical stretchability of connected Au@SEBS films by self-adhesion or TCIC. **e** The electrical stability of TCIC connected Au@SEBS and commercial Cu@PI, which simulates PI PCBs. **f** The electrical stretchability of TCIC-connected striped EGaIn@PDMS films. The films could not be connected without MTPs. **g** The electrical stability of TCIC connected striped EGaIn@PDMS. The resistance fluctuation was caused by the deformation of the liquid metal during stretching. The electrical stretchability of various electronic materials connected to **h**, Au@SEBS, **i** EGaIn@PDMS by TCIC.

regardless of the fluctuation caused by the deformation of liquid metal (Fig. 4g). The mechanical properties of the connections also tolerated cyclic stretching (Fig. S15), indicating the robustness of TCIC.

The electrical stretchability of combinations between stretchable and flexible/rigid conductors was measured (Fig. 4h and i). They all exhibited certain electrical stretchability, and the combination of stretchable conductors and commercial Cu@PI could endure cyclic bending and twisting (Fig. S16), confirming the universality of TCIC. For several most encountered conductive materials in electronics, Sn, Cu, and Au, the electrical stretchability all reached more than 40% strain. For Au@SEBS samples, the stretchability was limited by the Au-SEBS interface in the stretchable conductor (Fig. S17). Unlike Au@SEBS, EGaIn@PDMS samples had better conductivity, but their mechanical failure occurred earlier than electrical failure (Fig. S18). The selection between these two stretchable conductors should be done considering the practical requirements of the connections. The above results confirmed the universality of TCIC and the good electrical stretchability and stability of TCIC-connected electronics.

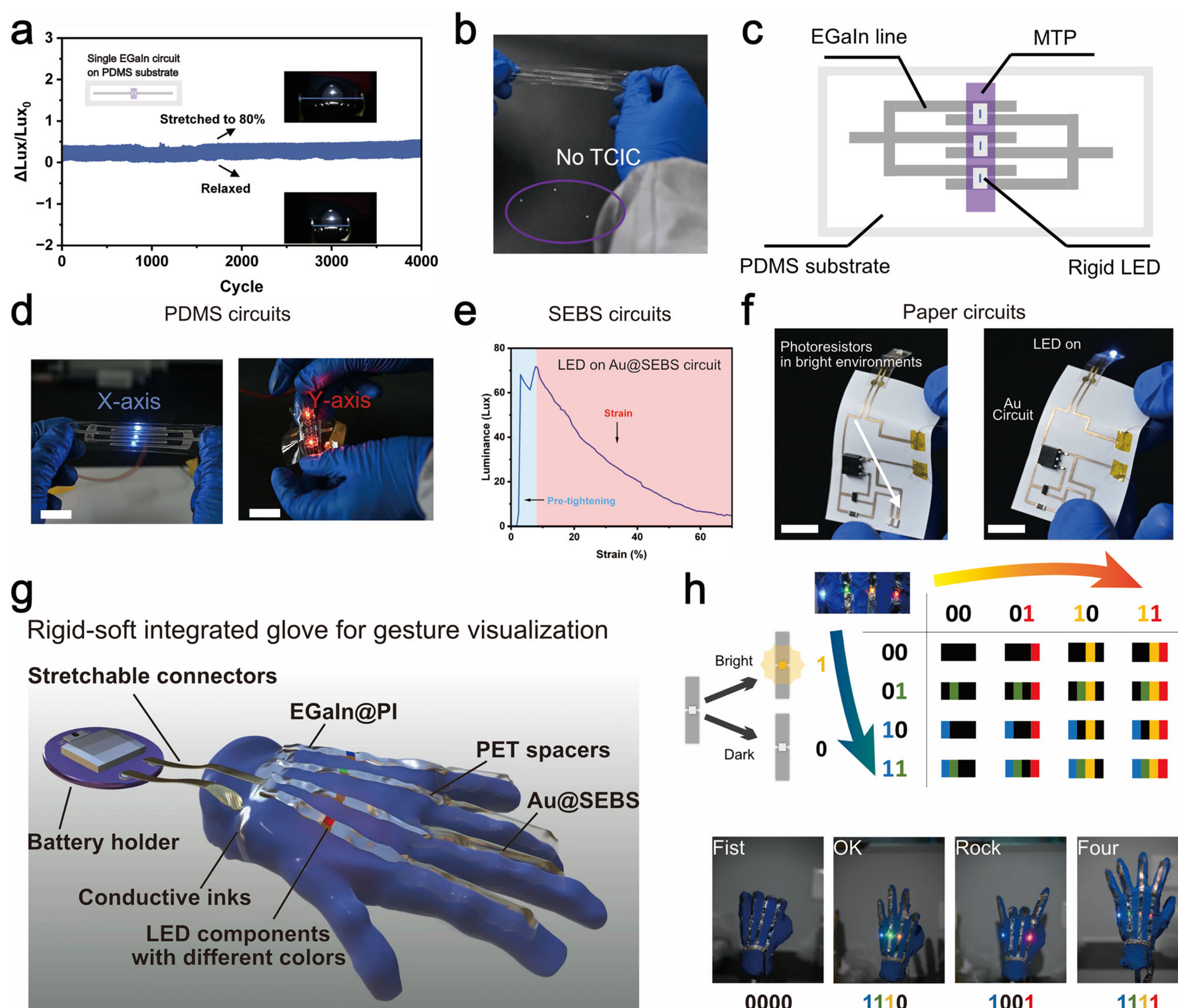

Fig. 5 | Flexible hybrid electronics constructed through TCIC. a Relative change in light intensity of an LED mounted on EGaIn@PDMS circuit by TCIC during cyclic stretching for 4000 cycles at 80% strain. The LED became brighter when being stretched as the contact area between LED pins and liquid metal increased after deformation. **b** LEDs were unable to stay on EGaIn@PDMS without TCIC treatment. **c** Schematic of the stretchable LED circuits on EGaIn@PDMS. **d** The TCIC-mounted LEDs could endure large strain during both the X- and Y-axis stretching. Scale bar: 3 cm. **e** Relative change in light intensity of an LED mounted on Au@SEBS circuit by TCIC. **f** A paper-based photoresistor-controlled flexible device. Scale bar: 1 cm. **g** Illustration of the gesture visualizing glove integrated from various soft/rigid units by TCIC. **h** Coding of the four colored lights on the gloves and four representative gestures with their corresponding codes.

Comparison between TCIC and other recently reported stretchable connections[41,43–46] was summarized in Table S1. TCIC had good mechanical durability and electrical stability; its fabrication and application were also one of the simplest. Most importantly, TCIC was applicable to most materials encountered in flexible electronics, endowing it with excellent universality. TCIC was also compared to commercial ACF, silver paste, and other reported ACFs[47–50] (Fig. S19 and Table S2), showing its advantages in convenience and performance.

Applications of TCIC in flexible hybrid electronics

TCIC was mild, fast, and universal for most materials used in electronics, which made it possible to integrate rigid electronic components with stretchable units quickly and stably for the fabrication of flexible hybrid devices. To illustrate the convenience and performance of TCIC, stretchable circuits on various flexible substrates were fabricated. Due to the excellent electrical stretchability of EGaIn@PDMS, circuits on PDMS exhibited satisfactory performance. TCIC-integrated LED on EGaIn@PDMS could be stretched to more than 80% strain while still lighting brightly (Movie S1). The TCIC-mounted LED was stable and could withstand more than 4000 stretching cycles without decay in light luminance (Fig. 5a). On the contrary, the attached LED on EGaIn@PDMS under the same conditions without MTP would easily detach from the circuits (Fig. 5b and Movie S2). Based on the EGaIn@PDMS, stretchable circuits with multiple LED sites were fabricated (Fig. 5c). The circuits exhibited excellent stretchability along different directions (Fig. 5d). Even when the LEDs were pulled up by a tweezer and shaken violently, the TCIC-mounted LED circuits would not fail and kept their light-emitting functions (Movie S2). The integration of LED with EGaIn@PDMS circuits confirmed the stability and high performance of TCIC in manufacturing flexible hybrid devices.

Au@SEBS circuits were also fabricated by TCIC. As shown in Fig. 5e, the light of LED on Au@SEBS decayed significantly when being stretched due to the increased resistance of Au@SEBS at the edges of the soft-rigid interfaces. The overall stretchability could be improved by constructing stable rigid islands via TCIC (Fig. S20), exhibiting the versatile application strategies of TCIC.

To further prove the versatility of TCIC, paper, a common and cheap substrate, was used for fabricating flexible circuits. The circuits could be directly drawn on paper by conductive inks, such as copper and silver paints.

Without any soldering process, LEDs were mounted on paper circuits by TCIC and could withstand twisting or bending (Fig. S21a and Movie S3). For more complicated and precise circuits, the conductive lines were produced by thermal vapor deposition of Au on papers with masks. A circuit was fabricated on paper and linked to an LED on Au@SEBS (Fig. S21b) with all interfaces connected by TCIC. The circuit had a photoresistor as control (Movie S4). This TCIC-integrated flexible hybrid device could function under deformation (Fig. 5f), validating the versatility of TCIC.

Finally, a multi-materials integrated gesture-visualizing glove was designed and fabricated with the entire system connected by TCIC. The glove was composed of multiple components and units, including the substrate nitrile glove, EGaIn, PI, Au@SEBS, PET, conductive silver paste, LED components, and a rigid battery holder unit (Fig. 5g). LEDs were mounted on EGaIn@PI by TCIC as LED rigid stripes, which were attached to the glove by TCIC. The finger direction of EGaIn@PI was connected to a hollow PET frame and Au@SEBS by TCIC (Fig. S22a). When the finger bends, the adhered Au@SEBS would be stretched with increased resistance, leading to open circuit and function as a switch that senses finger bending (Fig. S22b). The rest circuits on the glove were drawn by a conductive silver paste and connected to the battery holder through stretchable Au@SEBS by TCIC. The whole hybrid device was integrated by TCIC from the above-mentioned materials and units. Four LEDs with distinct colors were connected to four fingers and were ON when the fingers were straight. The colors of the lights indicated the position of the LED and were used for coding the gestures; thus, they could be recognized even in the dark (Fig. 5h and Fig. S23a). The distinct colors made it possible to distinguish the codes better, for instance, codes from single-colored LEDs would be indistinguishable for 0011, 0110, and 1100. The gesture visualization by the glove was also achieved on a human hand (Movie S5), and the gestures could be speculated by the lights in the dark (Fig. S23b). The applications of TCIC in the fabrication of multiple material/unit devices have further proved its stability, universality, convenience, and practicability in flexible hybrid electronics.

Discussion

Universal stretchable connections for flexible hybrid electronics were realized by thiol click interfacial connection (TCIC), which was simple but could stably and conveniently connect most materials and components used in flexible electronics. TCIC included a surface modification step and an interfacial covalent reaction step with multi-thiol polymers. The thiol-Au bonds and thiol-ene click reactions at interfaces provided robust mechanical connections between stretchable and flexible/rigid materials. The "welded" SEBS rubber and metals could withstand tensile strains over 250% with interfacial toughness over 200 N/m. The ultrathin MTP layer guaranteed anisotropic conductivity of the connections, achieving electrical stretchability over 50% between Au@SEBS and metals used in electronics. TCIC also exhibited high stability, the connected EGaIn@PDMS stretchable conductors kept excellent conductivity during and after 10,000 continuous stretching cycles to 60% strain. Moreover, the operations of TCIC were simple and the conditions were mild (below 60 °C) with self-strengthening properties at rt. Benefiting from the universality of TCIC, it was used to fabricate hybrid devices that integrate both soft and rigid units. Stretchable circuits were fabricated on PDMS and SEBS with mounted electronic components, and flexible devices were manufactured on papers and gloves, highlighting the versatility and robustness of TCIC. These characteristics of TCIC endowed stretchable connections with enormous potential in the fabrication and integration of multi-material flexible hybrid electronic devices.

Methods

Materials

Pentaerythritol tetrakis(3-mercapto-propionate) (PETMP, purity 95%) and EGaIn (Ga 75.5%/In 24.5%, purity 99.99%) were purchased from Sigma-Aldrich. Poly(ethylene glycol) diacrylate (PEGDA, Mw = 700 g/mol) was purchased from Aladdin Scientific. Sodium ethoxide (EtONa, purity 98%) and $CDCl_3$ (purity 99.8%) were purchased from J&K Scientific Ltd. 3-(trimethoxysilyl)propyl acrylate (purity 99%) was purchased from Macklin Reagent. Organic solvents were purchased from Chinasun. Polydimethylsiloxane (PDMS, SYLGARD 184) was the product of Dow Inc. Styrene ethylene butylene styrene (SEBS, H1221) was the product of Tuftec. Polyethylene glycol terephthalate (PET) was PP2910 produced by 3 M. Gold for thermal vapor deposition was purchased from ZhongNuo Advanced Material (Beijing) Technology Co., Ltd., with a purity of 99.999%. Polyimide (PI), paper (with smooth surfaces), electronics components, and other metal sheets were common commercial products. All the materials were used without further purification.

Fabrication of stretchable substrates and conductors

PDMS films (thickness ~100 μm) were prepared by spin-coating the PDMS precursor (curing ratio 10:1) onto a fluorinated silica plate at 1000 rpm for 15 seconds and then cured in an oven at 80 °C for 2 hours. SEBS films (thickness ~150 μm) were prepared by casting 20 mL of SEBS solution (13%wt in toluene) into a glass mold (round, diameter ~12 cm) and slowly removing the solvent by evaporation at rt. Metal deposition was done by electron beam evaporation with a Kurt J Lesker PVD75, at a rate of 0.5 Å/s for all samples. For Au@SEBS, a 45 nm thick Au layer was evaporated on the SEBS film. For Au@PDMS, 5 nm Cr was first evaporated on the PDMS film, followed by a 70 nm Au layer. The thickness of the Au layer on the paper substrate was 100 nm, and on the PET substrates was 70 nm. The circuit patterns were realized by using masks with the desired patterns. For EGaIn@PDMS, a patterned PET mask was placed on the top of the PDMS film, and EGaIn was coated by rubbing as reported in a previous article[51].

Synthesis of multi-thiol polymer (MTP)

2 g of PETMP and 830 μL of EtONa solution in ethanol (5 mg/mL) was added to a flask with 10 mL of chloroform, 2.57 g of PEGDA (molar ratio of PETMP: PEGDA = 1: 0.9) was added to a dropping funnel with 10 mL of chloroform. The PETMP solution was heated at 60 °C and stirred at 800 rpm, then the PEGDA solution was controlled to be added dropwise at a rate of 3 s a drop. The reaction continued for 2 h and was quenched by adding water. The reaction mixture was washed with water to remove the NaOH and ethanol, dried, and rotary evaporated to remove the chloroform solvent. The product MTP was not further purified. Air was not purposely avoided during the synthesis of MTP. The molecular weight of MTP was characterized by GPC(PL-GPC220). ^{1}HNMR were measured in $CDCl_3$ solutions by a Bruker AVANCEIII HD-400 NMR spectrometer at 298 K.

Thiol click interfacial connection (TCIC) process

The surface of the target material or unit was first treated with plasma (SAT-5D) at 90 W for 30 seconds. Then it was placed in a vacuum dryer containing 20 μL of 3-(trimethoxysilyl)propyl acrylate (dropped on a glass slide or petri dish). The vacuum dryer was evacuated to around 0.05 bar and left at rt for overnight. Then the surfaces of the target material or unit were ready for interfacial reactions. The water contact angle was tested on DataPhysics OCA to observe changes in surface properties. A typical MTP solution was prepared as follows: 100 mg MTP was completely dissolved in 1 mL of acetone, and then 32 μL of EtONa solution in ethanol (5 mg/mL) was added. The solution was shaken well and ready for use. A syringe with flat flat-head needle was used to spread the MTP solution on the target surfaces. The surfaces were then contacted and placed at the desired temperature for TCIC. For comparison, the controlled conditions (60 °C reaction for 1.5 h with 0.5 kPa pressure applied) were realized by placing an adequate weight (water in a container with a flat bottom) on the connection area.

Characterization

For AFM images, height and current mapping were measured using Bruker Dimension ICON. Raman spectra were recorded by a Horiba HR800. MTP was coated on Au@SEBS to characterize the formation of S-Au bonds. MTP was encapsulated in a quartz tube with acetone to observe the change of -SH

and -S-S-. The microscopic images were observed using an optical microscope (Nikon Y-TV55). The transmittance was measured using a UV-VIS-NIR Spectrophotometer (PE750).

Mechanical characterization

The mechanical strength was measured by a mechanical tester (YH-9002) in tensile stretching mode. The stretching speeds were all fixed at 60 mm/min. Sandwiched tensile experiments of the carbon tape group used carbon double-sided tape (Nisshin 731) and were pressed with 0.5 kPa pressure at 60 °C for 1.5 h. The samples were then cut into strips with a width of 5 mm for tensile testing. The interfacial toughness of soft-soft interfaces was measured by 180° peeling tests with 10 mm width of samples. The interfacial toughness of soft-flexible/rigid interfaces was measured by 90° peeling tests with 10 mm width of samples. The connection strength between rigid materials (Cu and Au@Cu) was measured by lap shear tests with a 10 mm × 10 mm overlapping area. The mechanical stretchability and electrical stretchability were measured in lap shear mode with a 10 mm × 10 mm overlapping area.

Electrical characterization

The electrical resistance was measured by a DMM6500 6.5-digit multimeter. Liquid metal lines were drawn on samples for better contact with the wires from the multimeter. The stretching rate for electrical stretchability tests was 10 mm/min. The cycle stability of TCIC-connected Au@SEBS and commercial PI PCB was recorded after reaching a stable state (after about 200 cycles) due to the continuously decreasing resistance of Au@SEBS in the initial stretching and releasing cycles. The luminance of the LED with EGaIn@PDMS and Au@SEBS was recorded by a UNI-T ut382 in a dark box to avoid the influence of environmental light.

Data availability

The authors declare that the data supporting the findings of this study are available within the paper and its Supplementary Information files. Should any raw data files be needed in another format, they are available from the corresponding author upon reasonable request.

Received: 14 April 2025; Accepted: 30 June 2025;
Published online: 09 July 2025

References

1. Byun, S. H. et al. Mechanically transformative electronics, sensors, and implantable devices. *Sci. Adv.* **5**, eaay0418 (2019).
2. Li, H., Tang, Z., Liu, Z. & Zhi, C. Evaluating flexibility and wearability of flexible energy storage devices. *Joule* **3**, 613–619 (2019).
3. Zhang, Z. et al. Eco-friendly, self-healing hydrogels for adhesive and elastic strain sensors, circuit repairing, and flexible electronic devices. *Macromolecules* **52**, 2531–2541 (2019).
4. Cao, C. et al. Mitigating the overheat of stretchable electronic devices via high-enthalpy thermal dissipation of hydrogel encapsulation. *Adv. Mater.* **36**, e2401875 (2024).
5. Rogers, J. A., Someya, T. & Huang, Y. Materials and mechanics for stretchable electronics. *Science* **327**, 1603–1607 (2010).
6. Zhuang, Q. et al. Permeable, three-dimensional integrated electronic skins with stretchable hybrid liquid metal solders. *Nat. Electron.* **7**, 598–609 (2024).
7. Zhang, Z. et al. High-brightness all-polymer stretchable LED with charge-trapping dilution. *Nature* **603**, 624–630 (2022).
8. Zhang, S., Ke, X., Jiang, Q., Ding, H. & Wu, Z. Programmable and reprocessable multifunctional elastomeric sheets for soft origami robots. *Sci. Robot.* **6**, eabd6107 (2021).
9. Park, S. et al. Self-powered ultra-flexible electronics via nano-grating-patterned organic photovoltaics. *Nature* **561**, 516–521 (2018).
10. Brasier, N. et al. Applied body-fluid analysis by wearable devices. *Nature* **636**, 57–68 (2024).
11. Chen, S. et al. Ultrahigh strain-insensitive integrated hybrid electronics using highly stretchable bilayer liquid metal based conductor. *Adv. Mater.* **35**, e2208569 (2023).
12. Duan, J., Liang, X., Guo, J., Zhu, K. & Zhang, L. Ultra-stretchable and force-sensitive hydrogels reinforced with chitosan microspheres embedded in polymer networks. *Adv. Mater.* **28**, 8037–8044 (2016).
13. Lei, Z. & Wu, P. A highly transparent and ultra-stretchable conductor with stable conductivity during large deformation. *Nat. Commun.* **10**, 3429 (2019).
14. Ershad, F. et al. Ultra-conformal drawn-on-skin electronics for multifunctional motion artifact-free sensing and point-of-care treatment. *Nat. Commun.* **11**, 3823 (2020).
15. Gao, W., Ota, H., Kiriya, D., Takei, K. & Javey, A. Flexible electronics toward wearable sensing. *Acc. Chem. Res.* **52**, 523–533 (2019).
16. Guo, R. et al. Semiliquid metal enabled highly conductive wearable electronics for smart fabrics. *ACS Appl. Mater. Interfaces* **11**, 30019–30027 (2019).
17. Yamamoto, Y. et al. Efficient skin temperature sensor and stable gel-less Sticky ECG sensor for a wearable flexible healthcare patch. *Adv. Healthc. Mater.* **6**, 1700495 (2017).
18. Yuk, H. et al. Dry double-sided tape for adhesion of wet tissues and devices. *Nature* **575**, 169–174 (2019).
19. Kim, J. et al. Stretchable silicon nanoribbon electronics for skin prosthesis. *Nat. Commun.* **5**, 5747 (2014).
20. Yang, Y. & Gao, W. Wearable and flexible electronics for continuous molecular monitoring. *Chem. Soc. Rev.* **48**, 1465–1491 (2019).
21. Liu, Y., Pharr, M. & Salvatore, G. A. Lab-on-skin: a review of flexible and stretchable electronics for wearable health monitoring. *ACS Nano* **11**, 9614–9635 (2017).
22. Maheshwari, V. & Saraf, R. Tactile devices to sense touch on a par with a human finger. *Angew. Chem. Int. Ed.* **47**, 7808–7826 (2008).
23. Tang, L., Wang, H., Ren, J. & Jiang, X. Highly robust soft-rigid connections via mechanical interlocking for assembling ultra-stretchable displays. *npj Flex. Electron* **8**, 50 (2024).
24. Minev, I. R. et al. Biomaterials. Electronic dura mater for long-term multimodal neural interfaces. *Science* **347**, 159–163 (2015).
25. Viventi, J. et al. A conformal, bio-interfaced class of silicon electronics for mapping cardiac electrophysiology. *Sci. Transl. Med.* **2**, 24ra22 (2010).
26. Cui, G. P. et al. 3D-printed Bi(2)Te(3)-based Thermoelectric Generators for Energy Harvesting and Temperature Response. *ACS Appl. Mater. Interfaces* **16**, 35353–35360 (2024).
27. Ji, S. & Chen, X. Enhancing the interfacial binding strength between modular stretchable electronic components. *Natl Sci. Rev.* **10**, nwac172 (2023).
28. Wu, B., Wu, T., Huang, Z. & Ji, S. Advancing flexible sensors through on-demand regulation of supramolecular nanostructures. *ACS Nano* **18**, 22664–22674 (2024).
29. Chen, Z., Zhang, G., Luo, Y. & Suo, Z. Rubber-glass nanocomposites fabricated using mixed emulsions. *Proc. Natl Acad. Sci. Usa.* **121**, e2322684121 (2024).
30. Naserifar, N., LeDuc, P. R. & Fedder, G. K. Material gradients in stretchable substrates toward integrated electronic functionality. *Adv. Mater.* **28**, 3584–3591 (2016).
31. Sun, B. et al. Gradient modulus strategy for alleviating stretchable electronic strain concentration. *Adv. Funct. Mater.* **34**, 2410676 (2024).
32. Yang, J. C. et al. Geometrically engineered rigid island array for stretchable electronics capable of withstanding various deformation modes. *Sci. Adv.* **8**, eabn3863 (2022).
33. Liu, Y., He, K., Chen, G., Leow, W. R. & Chen, X. Nature-inspired structural materials for flexible electronic devices. *Chem. Rev.* **117**, 12893–12941 (2017).
34. Lim, H. S., Kim, S.-N., Lim, J. A. & Park, S.-D. Low temperature-cured electrically conductive pastes for interconnection on electronic devices. *J. Mater. Chem.* **22**, 20529 (2012).

35. Ozutemiz, K. B., Wissman, J., Ozdoganlar, O. B. & Majidi, C. EGaIn–metal interfacing for liquid metal circuitry and microelectronics integration. *Adv. Mater. Interfaces* **5**, 1701596 (2018).
36. Hirsch, A., Dejace, L., Michaud, H. O. & Lacour, S. P. Harnessing the rheological properties of liquid metals to shape soft electronic conductors for wearable applications. *Acc. Chem. Res.* **52**, 534–544 (2019).
37. Soh, E. J. H. et al. AFM manipulation of EGaIn microdroplets to generate controlled, on-demand contacts on molecular self-assembled monolayers. *ACS Nano* **16**, 14370–14378 (2022).
38. Hwang, H. et al. Stretchable anisotropic conductive film (S-ACF) for electrical interfacing in high-resolution stretchable circuits. *Sci. Adv.* **7**, eabh0171 (2021).
39. Park, Y. G. et al. Self-healable, recyclable anisotropic conductive films of liquid metal-gelatin hybrids for soft electronics. *Adv. Electron. Mater.* **8**, 2101034 (2022).
40. Jiang, Z. et al. A 1.3-micrometre-thick elastic conductor for seamless on-skin and implantable sensors. *Nat. Electron.* **5**, 784–793 (2022).
41. Jiang, Y. et al. A universal interface for plug-and-play assembly of stretchable devices. *Nature* **614**, 456–462 (2023).
42. Luo Y.-R. *Comprehensive Handbook of Chemical Bond Energies*. CRC Press (2007).
43. Dou, J., Tang, L., Mou, L., Zhang, R. & Jiang, X. Stretchable conductive adhesives for connection of electronics in wearable devices based on metal-polymer conductors and carbon nanotubes. *Compos. Sci. Tech.* **197**, 108237 (2020).
44. Zhang, A., Maly, J. & Ameri, S. K. Hetero phase nanocomposite based posture sensor with stretchable connector-sensor interface. *Sens. Actuat. A: Phys.* **378**, 115811 (2024).
45. Park, D. et al. Stretchable anisotropic conductive film with position-registered conductive microparticles used for strain-insensitive ionic interfacing in stretchable ionic sensors. *Adv. Funct. Mater.* **34**, 2408902 (2024).
46. Yoon, H., Jeong, S., Lee, B. & Hong, Y. A site-selective integration strategy for microdevices on conformable substrates. *Nat. Electron.* **7**, 383–395 (2024).
47. Haque, A. B. M. T. et al. Electrically conductive liquid metal composite adhesives for reversible bonding of soft electronics. *Adv. Funct. Mater.* **34**, 2304101 (2024).
48. Pozarycki, T. A., Zu, W., Wilcox, B. T. & Bartlett, M. D. A flexible and electrically conductive liquid metal adhesive for hybrid electronic integration. *Adv. Funct. Mater.* **34**, 2313567 (2024).
49. Jeong, K. et al. A Sub-Micron-Thick stretchable adhesive layer for the lamination of arbitrary elastomeric substrates with enhanced adhesion stability. *Chem. Eng. J.* **429**, 132250 (2022).
50. Huynh, V. L., Aasmundtveit, K. E. & Nguyen, H. V. Enabling low pressure, low temperature, and particle control for anisotropic conductive adhesives. *Adv. Mater. Technol.* **9**, 2400262 (2024).
51. Yuan, B., Sun, X., Wang, Q. & Wang, H. Direct fabrication of liquid-metal multifunctional paper based on force-responsive adhesion. *Cell Rep. Phys. Sci.* **4**, 101419 (2023).

Acknowledgements

This work is supported by Collaborative Innovation Center of Suzhou Nano Science & Technology; the 111 Project; Innovative Center for Molecular Science of Surface and Interface, Soochow University; Suzhou Key Laboratory of Surface and Interface of Intelligent Matter (Grant no. SZS2022011); the Gusu Innovation and Entrepreneurship Talent Program - Major Innovation Team (ZXD2023002); Basic Research Program of Jiangsu Province (BK20240826); National Natural Science Foundation of China (52473218, U24A20496).

Author contributions

S.J. and L.C. conceived and designed the experiments. Y.Z., Q.R., T.L., H.Q., R.Z. and S.W. performed the experiments. Y.Z., Q.R. and S.J. analyzed the data. Y.Z., S.J. and L.C. wrote the manuscript with contributions from all authors. All authors reviewed the manuscript.

Competing interests

The authors declare no competing interests.

Additional information

Supplementary information The online version contains supplementary material available at https://doi.org/10.1038/s41528-025-00449-w.

Correspondence and requests for materials should be addressed to Lifeng Chi or Shaobo Ji.

Reprints and permissions information is available at http://www.nature.com/reprints

Publisher's note Springer Nature remains neutral with regard to jurisdictional claims in published maps and institutional affiliations.

Open Access This article is licensed under a Creative Commons Attribution-NonCommercial-NoDerivatives 4.0 International License, which permits any non-commercial use, sharing, distribution and reproduction in any medium or format, as long as you give appropriate credit to the original author(s) and the source, provide a link to the Creative Commons licence, and indicate if you modified the licensed material. You do not have permission under this licence to share adapted material derived from this article or parts of it. The images or other third party material in this article are included in the article's Creative Commons licence, unless indicated otherwise in a credit line to the material. If material is not included in the article's Creative Commons licence and your intended use is not permitted by statutory regulation or exceeds the permitted use, you will need to obtain permission directly from the copyright holder. To view a copy of this licence, visit http://creativecommons.org/licenses/by-nc-nd/4.0/.

© The Author(s) 2025